

Glycosylated Star-Shaped Conjugated Oligomers for Targeted Two-Photon Fluorescence Imaging

Guan Wang,^[a, b] Xinhai Zhang,^[c] Junlong Geng,^[a] Kai Li,^[c] Dan Ding,^[a] Kan-Yi Pu,^[a] Liping Cai,^[a] Yee-Hing Lai,^{*, [b]} and Bin Liu^{*, [a, c]}

Abstract: A glucopyranose functionalized star-shaped oligomer, *N*-tris{4,4',4''-[(1*E*)-2-(2-[(*E*)-2-[4-(benzo[*d*]thiazol-2-yl)phenyl]vinyl)-9,9-bis(6-2-amido-2-deoxy-1-thio-β-D-glucopyranose-hexyl)-9*H*-fluoren-7-yl)vinyl]phenyl}phenylamine (TVFVBN-S-NH₂), is synthesized for two-photon fluorescence imaging. In water, TVFVBN-S-NH₂ self-assembles into nanoparticles with an average diameter of ~49 nm and shows a fluorescence quantum yield of 0.21. Two-photon fluorescence measurements reveal that

TVFVBN-S-NH₂ has a two-photon absorption cross-section of ~1100 GM at 780 nm in water. The active amine group on the glucopyranose moiety allows further functionalization of TVFVBN-S-NH₂ with folic acid to yield TVFVBN-S-NH₂FA with similar optical and physical properties as those for TVFVBN-S-NH₂. Cellular imaging

studies reveal that TVFVBN-S-NH₂FA has increased uptake by MCF-7 cells relative to that for TVFVBN-S-NH₂, due to specific interactions between folic acid and folate receptors on the MCF-7 cell membrane. This study demonstrates the effectiveness of glycosylation as a molecular engineering strategy to yield water-soluble materials with a large two-photon absorption (TPA) cross-section for targeted cancer-cell imaging.

Keywords: fluorescence • glucopyranose • oligomers • self-assembly • targeted imaging

Introduction

Two-photon microscopy (TPM), which offers several advantages over conventional one-photon confocal laser scanning microscopy (CLSM), such as intrinsic high 3D resolution, deeper penetration, less photodamage and less photobleaching, has emerged as a powerful technology for non-invasive biological imaging.^[1] The advancement of TPM imaging is highly dependent on the design and synthesis of highly fluorescent two-photon absorbing materials. Although quantum dots (QDs) as two-photon absorbing materials offer many

merits, such as high photostability and high brightness, the intrinsic toxicity of QDs in the oxidative environment limits their applications in long-term monitoring of cellular events.^[2] On the other hand, fluorescent proteins used for TPM imaging generally show small two-photon absorption (TPA) cross-sections (δ) of less than 300 GM.^[3] In addition, their drawbacks related to maturation and monomeric state were reported to show severe cytotoxicity effects.^[4] The shortcomings of QDs and fluorescent proteins have motivated researchers to develop alternative TPA chromophores, such as organic π -conjugated materials for two-photon fluorescence imaging applications.

Organic π -conjugated materials with traditional linear push-pull structures (donor-acceptor, D-A) generally exhibit smaller TPA cross-sections (δ) relative to those for quadrupolar (D-A-D or A-D-A) and octupolar systems.^[5] However, star-shaped and dendritic chromophores, such as three-branched octupolar structures, could bring excitonic coupling between the dipolar branch and the central core to induce large TPA δ values.^[6] Although materials with a TPA δ larger than 2000 GM have been reported,^[5] most of them are only soluble in organic solvents with limited biological applications. In addition, water-soluble derivatives of these TPA materials generally show a significantly decreased δ value relative to their neutral counterparts in organic solvents.^[7] To address this problem, we recently found that integration of a glucose moiety with a star-shaped π -conjugated oligomer is an effective strategy to yield a robust water-soluble TPA material (structure shown as TFBS) with high

[a] G. Wang, J. Geng, Dr. D. Ding, Dr. K.-Y. Pu, Dr. L. Cai, Prof. B. Liu
Department of Chemical and Biomolecular Engineering
National University of Singapore
4 Engineering Drive 4, National University of Singapore
Singapore 117576 (Singapore)
Fax: (+65)6779-1936
E-mail: cheliub@nus.edu.sg

[b] G. Wang, Prof. Y.-H. Lai
Department of Chemistry
National University of Singapore
3 Science Drive 3, National University of Singapore
Singapore 117543 (Singapore)
E-mail: chmlaiyh@nus.edu.sg

[c] Dr. X. Zhang, Dr. K. Li, Prof. B. Liu
Institute of Materials Research and Engineering
3 Research Link, Singapore 117602 (Singapore)

Supporting information for this article is available on the WWW under <http://dx.doi.org/10.1002/chem.201200849>: NMR spectra, MALDI-TOF mass spectra.

phosphate salt diethyl [4-(benzo[*d*]thiazol-2-yl)phenyl]methylphosphonate (**3**) in 84% yield upon heating with triethylphosphite at 180 °C for 3 h.^[18] Tris(4-formylphenyl)amine (**4**) was synthesized from triphenylamine and POCl₃ by using a modified procedure from a literature report.^[19] Amine **4** was then treated with NaBH₄ to yield tris(4-hydroxymethylphenyl)amine (**5**). Further bromination of **5** with HBr gas afforded tris(4-bromomethylphenyl)amine (**6**), which upon heating with triethylphosphite at 120 °C yielded tris(4-diethylphosphonatemethylphenyl)amine (**7**) in an overall yield of 67% for three steps. 9,9-Bis(6-bromoethyl)-9*H*-fluorene-2,7-dicarbaldehyde (**8**) was synthesized in 39% yield from 2,7-dibromo-9,9-bis(6-bromoethyl)-9*H*-fluorene by using *n*BuLi and anhydrous DMF at -78 °C. Coupling one equivalent of **3** with **8** under Horner–Emmons conditions afforded monoaldehyde **9** in 35% yield. Horner–Emmons coupling between three equivalents of **7** and **9** gave TVFVBN in 65% yield. The correct structure of TVFVBN was affirmed by NMR spectroscopy and MALDI-TOF mass spectroscopy (see Figures S1a and S1b in the Supporting Information).

Further reaction between TVFVBN and 2-acetamido-2-deoxy-1-thio-β-D-glucopyranose 3,4,6-triacetate with K₂CO₃ as the base afforded TVFVBN-S-NHAc in 80% yield. The disappearance of the triplet at 3.29 ppm (CH₂Br) in the ¹H NMR spectrum (see Figure S2a in the Supporting Information) of TVFVBN-S-NHAc indicates 100% attachment of glucopyranose onto TVFVBN. The correct molecular mass was confirmed by MALDI-TOF spectroscopy (see Figure S2b in the Supporting Information). Hydrolysis of TVFVBN-S-NHAc in the presence of hydrazine under reflux conditions^[20] afforded TVFVBN-S-NH₂ in 94% yield after dialysis and freeze drying. The ¹H NMR spectrum for TVFVBN-S-NH₂ is shown in Figure S3 in the Supporting Information. The singlet for acetyl groups from the ¹H NMR spectrum of TVFVBN-S-NHAc is almost unobservable, which indicates the successful deacetylation of NHAc and OAc groups to NH₂ and OH, respectively. The folic acid conjugation was conducted by using *N,N*-dicyclohexylcarbodiimide (DCC)/*N*-hydroxysuccinimide (NHS) at a molar ratio of 1:10 for folic acid and TVFVBN-S-NH₂ to give folic acid functionalized TVFVBN-S-NH₂FA. After purification by dialysis with a 3.5 kDa molecular weight cut-off membrane against Mill-Q water for two days, TVFVBN-S-NH₂FA was obtained in a quantitative yield as an orange powder after freeze drying. The ¹H NMR spectrum of TVFVBN-S-NH₂FA is shown in Figure S4 in the Supporting Information.

Self-assembly in water: The self-assembly behaviours of TVFVBN-S-NH₂ and TVFVBN-S-NH₂FA were studied by using dynamic light scattering (DLS). As shown in Figure 1, the mean diameter for TVFVBN-S-NH₂ in water is ~49 nm with a polydispersity of 0.23 (Figure 1a), whereas that for TVFVBN-S-NH₂FA is ~50 nm with a polydispersity of 0.27 (Figure 1b). The polydispersities for both (0.23 and 0.27) are less than 0.3, which indicates that they form nanoparticles that are medium-dispersed in water.^[21]

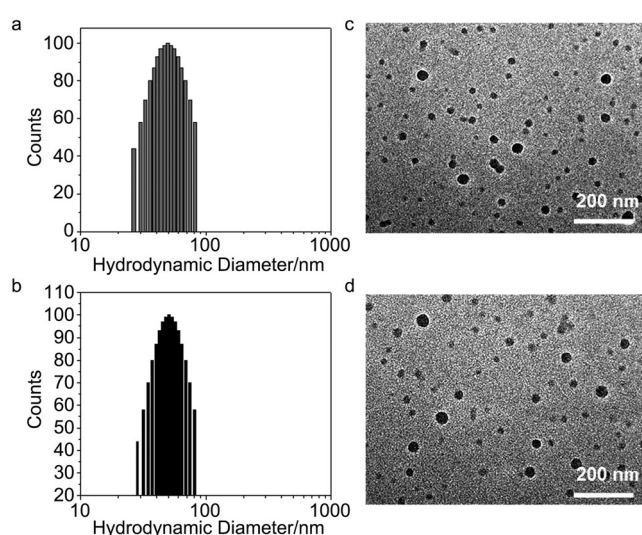


Figure 1. DLS spectra of 2 μm TVFVBN-S-NH₂ (a) and TVFVBN-S-NH₂FA (b) in water and TEM images of TVFVBN-S-NH₂ (c) and TVFVBN-S-NH₂FA (d) nanoparticles.

TEM was performed to study the morphology of the self-assembled nanoparticles. The samples were prepared by drop-coating of TVFVBN-S-NH₂ and TVFVBN-S-NH₂FA solutions (2 μm in water) onto a copper grid. As shown in Figure 1c and d, both TVFVBN-S-NH₂ and TVFVBN-S-NH₂FA form spherical nanoparticles with mean diameters of ~20 nm. The smaller size in TEM relative to those in DLS is due to the shrinking of samples when transformed into a dry state from solution.^[22] The fact that both TVFVBN-S-NH₂ and TVFVBN-S-NH₂FA have nearly the same nanoparticle size indicates that folic acid conjugation does not obviously change the self-assembly behaviour of TVFVBN-S-NH₂ in water. However, it is noteworthy that both TVFVBN-S-NH₂ and TVFVBN-S-NH₂FA are dissolved into the molecular level in DMSO with no DLS signals.

Linear optical properties: The UV/Vis absorption and PL spectra of TVFVBN in different solvents at a concentration of 2 μm are shown in Figure 2. The absorption spectra of

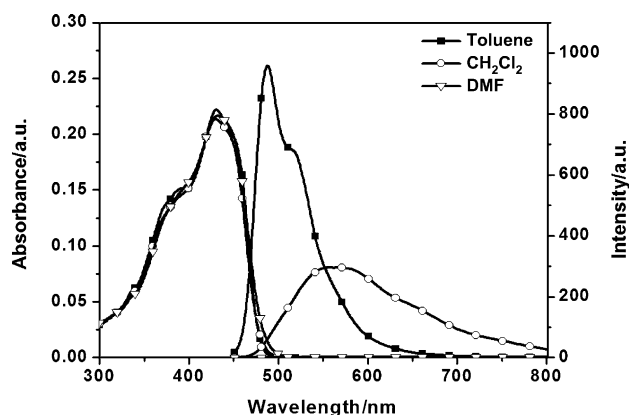


Figure 2. UV/Vis absorption and PL spectra of TVFVBN in toluene, dichloromethane and DMF.

TVFVBN in toluene, dichloromethane and dimethylformamide (DMF) have the same shape and maxima, which indicate that the ground state of TVFVBN is not sensitive to solvent polarity.^[23] On the other hand, the emission maximum of TVFVBN in toluene is at 486 nm, which is redshifted to 564 nm in dichloromethane. The quantum yields of TVFVBN in toluene and dichloromethane are 0.99 and 0.68, respectively, measured by using Rhodamine 6G in methanol as the reference. However, under the same experimental conditions, no fluorescence is observed for TVFVBN in DMF. Our previous molecular-orbital simulation indicates that charge transfer from electron-rich triphenylamine to electron-deficient benzothiazole units exists in the excited state.^[8] Similarly, the redshifted emission maxima and decreased fluorescence quantum yields with increased solvent polarity for TVFVBN are due to the charge-transfer characteristics of its excited state. As a result, bright greenish/blue and orange fluorescent colours are observed for the toluene and dichloromethane solutions of TVFVBN, whereas its DMF solution is not emissive (see Figure S5 in the Supporting Information).

The absorption and emission spectra of TVFVBN-S-NH₂ in DMSO and pure water are presented in Figure 3. The absorption spectra of TVFVBN-S-NH₂ in DMSO and water

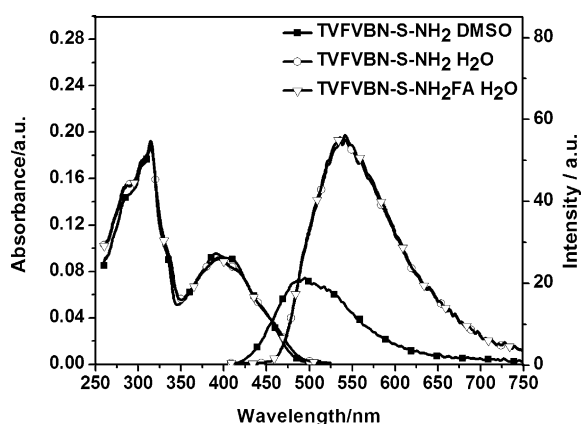


Figure 3. UV/Vis absorption and PL spectra of TVFVBN-S-NH₂ in DMSO and H₂O and TVFVBN-S-NH₂FA in H₂O.

are similar, with the maximum at 393 nm. The emission maxima of TVFVBN-S-NH₂ in DMSO and water locate at 494 and 542 nm, respectively. The quantum yield of TVFVBN-S-NH₂ in water is 0.21, which is substantially higher than that in DMSO (0.07). The higher quantum yield of TVFVBN-S-NH₂ in water relative to that in DMSO is ascribed to the formation of nanoparticles, as supported by the DLS and TEM measurements. In DMSO, TVFVBN-S-NH₂ is dissolved into the molecular level as aforementioned, and the charge-transfer between TVFVBN-S-NH₂ and DMSO quenches the fluorescence. However, the nanoparticles formed in water provide a hydrophobic microenvironment for TVFVBN-S-NH₂, which reduces its interaction with water for fluorescence quenching.^[22a] After conjugation

with folic acid, the optical properties of TVFVBN-S-NH₂FA are nearly the same as those for TVFVBN-S-NH₂, which indicate that folic acid conjugation does not change the linear optical properties of TVFVBN-S-NH₂ in water. As shown in Figure S5 in the Supporting Information, the aqueous solution of TVFVBN-S-NH₂ shows bright-yellow fluorescence, which indicates a high potential for optical applications.

TPA properties: The TPA spectra of TVFVBN in toluene and TVFVBN-S-NH₂ in water were collected by using a standard two-photon excited fluorescence (TPEF) technique with a femtosecond pulsed laser source.^[24] To avoid the interference on TPEF by laser excitation, TPA spectra were measured by starting at the wavelength at which each individual oligomer has nearly no emission. In addition, limited by the laser availability in our experiments, TVFVBN in toluene was investigated in the range from 740 to 900 nm, whereas TVFVBN-S-NH₂ in water was studied from 750 to 900 nm.

The TPA spectrum of TVFVBN in toluene (see Figure S6 in the Supporting Information) shows a maximum cross-section (δ) of 3031 GM at 820 nm. This value is \sim 500 GM larger than TFBN^[8] (2494 GM), which is ascribed to the increased coplanarity with an ethylene linker for TVFVBN. This δ value is also larger than those for octupolar tri-branched molecules when using triphenylamine as the core, with a fluorenyl-ethylene linker and SO₂CF₃ (2080 GM)^[6a] or CHO (1265 GM)^[25] as the peripheries, respectively. This agrees with the fact that an elongated conjugated backbone and a proper degree of intramolecular charge transfer (ICT) favour larger TPA δ values.^[26]

The TPA spectrum of TVFVBN-S-NH₂ in water is shown in Figure 4. The maximum TPA δ value is 1098 GM at 780 nm, giving an action cross-section value ($\eta\delta$) of 230 GM.

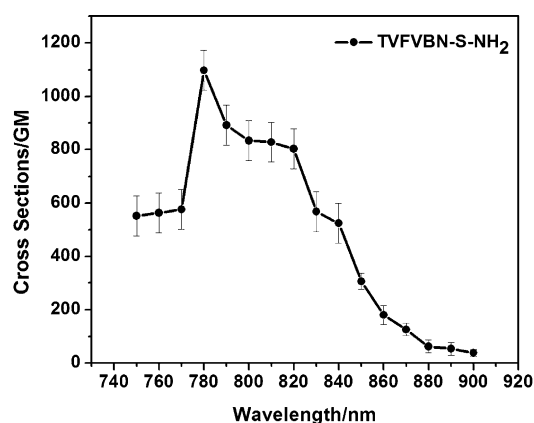


Figure 4. TPA cross-sections of TVFVBN-S-NH₂ in water.

As TVFVBN and TVFVBN-S-NH₂ share the same backbone, the decrease of the TPA δ value relative to that in toluene is due to the solvent effect, because water can influence the electronic structure of donor-acceptor chromophores through hydrogen bonding, which leads to a de-

creased ICT.^[7b] A further study of TVFVBN-S-NH₂FA under the same conditions yielded a similar $\eta\delta$ value (see Figure S7 in the Supporting Information). As a consequence, the large TPA $\eta\delta$ of TVFVBN-S-NH₂ in water would ensure a high brightness in two-photon biological imaging applications. Moreover, the $\lambda_{\text{max(TPA)}}$ of 780 nm makes TVFVBN-S-NH₂ more appealing for biological applications relative to TFBS, since excitation at longer wavelength can lead to less photodamage and photobleaching.

Targeted one- and two-photon fluorescence imaging: To demonstrate the potential of glycosylated materials in targeted cellular imaging, single (CLSM) and two-photon fluorescence (TPEF) cellular imaging of MCF-7 cancer cells were investigated with TVFVBN-S-NH₂FA and TVFVBN-S-NH₂. MCF-7 cancer cells are known to over express folate receptors, and, therefore, TVFVBN-S-NH₂FA with folate targeting ligands is expected to offer a higher uptake by MCF-7 cells relative to TVFVBN-S-NH₂. MCF-7 cells were incubated with TVFVBN-S-NH₂ and TVFVBN-S-NH₂FA at the molar concentration of 1 μM before fixation and image. As shown in Figure 5, both CLSM images of MCF-7 cells in-

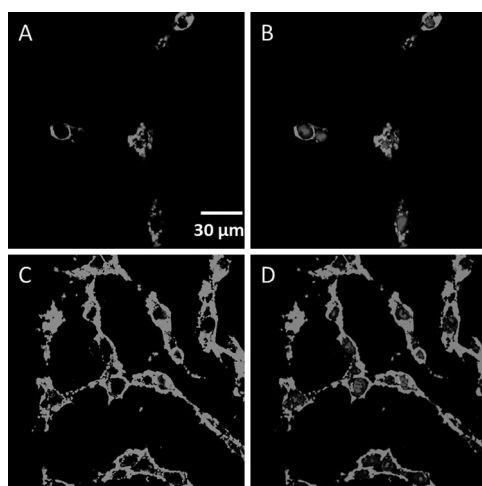


Figure 5. CLSM images of MCF-7 breast cancer cells after incubation with TVFVBN-S-NH₂ (a) and TVFVBN-S-NH₂FA (c); images a and c together with propidium iodide nucleus stain are shown in b and d. a–d share the same scale bar.

cubated with TVFVBN-S-NH₂ (Figure 5a) and TVFVBN-S-NH₂FA (Figure 5c) show green fluorescence. In addition, the fluorescence from Figure 5c is about three times (estimated by using ImageJ, Figure S8 in the Supporting Information) more intense relative to that from Figure 5a, which indicates the increased cellular uptake of TVFVBN-S-NH₂FA by MCF-7 cells. Figure 5b and d are the overlapped images with nuclei stained, which clearly indicate that both TVFVBN-S-NH₂ and TVFVBN-S-NH₂FA are localized in the cytoplasm of MCF-7 cells. The experiments have also been tested in living MCF-7 cells, which offered essentially similar results as those for fixed cells (see Figure S9 in the Supporting Information).

To confirm the folate receptor-mediated targeting effect of TVFVBN-S-NH₂FA, firstly, we studied the competitive effect of folic acid on the endocytosis of TVFVBN-S-NH₂FA on MCF-7 cells. As shown in Figure S10 in the Supporting Information, the fluorescence image of free folic acid pretreated MCF-7 cells shows lower intensity relative to that in Figure 5c. This indicates that the uptake of TVFVBN-S-NH₂FA is greatly inhibited by the free folic acid treatment, which effectively blocks the interaction between TVFVBN-S-NH₂FA and the folate receptor on the cell surface.^[10b] In addition, NIH/3T3 fibroblast normal cells, which lack a folate receptor on the cell membrane, were also used as a negative control. The CLSM images of NIH/3T3 cells treated with TVFVBN-S-NH₂FA and TVFVBN-S-NH₂ are shown in Figure S11 in the Supporting Information. The fluorescence intensities in Figure S11A (stained with TVFVBN-S-NH₂) and Figure S11C (stained with TVFVBN-S-NH₂FA) are comparable to each other, which are weaker than that in Figure 5c (estimated by using ImageJ, see Figure S12 in the Supporting Information). These data indicate the specific binding between TVFVBN-S-NH₂FA and the folate receptor on the cell surface, which shows the ability of TVFVBN-S-NH₂FA to discriminate folate-positive cancer cells from others.

The TPEF images MCF-7 cells incubated with TVFVBN-S-NH₂ and TVFVBN-S-NH₂FA are shown in Figure 6a and b, respectively. Green fluorescence was obtained in both images upon excitation at 800 nm with an average laser power of 10 mW. The fluorescence from Figure 6b is substantially brighter than that from Figure 6a, which is ascribed to the increased cellular uptake of TVFVBN-S-NH₂FA relative to TVFVBN-S-NH₂. In addition, the bright-green fluorescence from Figure 6b should benefit from the large TPA cross-section of TVFVBN-S-NH₂ in the 750–830 nm region (up to 1098 GM), which is substantially larger than a number of fluorescent probes designed for TPEF imaging applications.^[14c,27] These data clearly illustrate the potential of using TVFVBN-S-NH₂FA as a two-photon fluorescent probe for targeted TPEF cellular imaging.

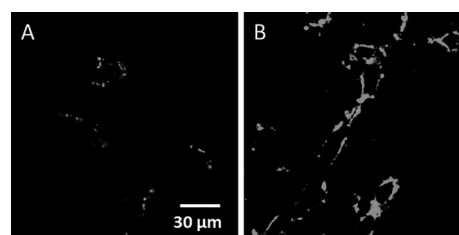


Figure 6. a) TPEF images of MCF-7 breast cancer cells after incubation with TVFVBN-S-NH₂ (a) and TVFVBN-S-NH₂FA (b). a and b share the same scale.

Cytotoxicity and photostability study: The cytotoxicity of TVFVBN-S-NH₂ and TVFVBN-S-NH₂FA was evaluated for MCF-7 cells by using a methylthiazolyldiphenyl-tetrazolium (MTT) cell viability assay. Figure S13 in the Supporting In-

formation shows the in vitro MCF-7 cell viabilities after being cultured with TVFVBN-S-NH₂ and TVFVBN-S-NH₂FA solution at concentrations of 1, 10 and 100 μM for 24, 48 and 72 h, respectively. Within the test period of time, the cell viabilities are close to 100% at 10 μM each (10 times the concentration used for imaging studies shown in Figure 5), which indicates the low cytotoxicity of both TVFVBN-S-NH₂ and TVFVBN-S-NH₂FA. When the concentration is increased to 100 μM, both oligomers exhibit slight cytotoxicity (the cell viabilities drop to ≈80%). These studies indicate that both oligomers are suitable for in vitro and in vivo cellular imaging studies. The changes in the CLSM and TPM images of MCF-7 cells treated with TVFVBN-S-NH₂FA before and after continuous laser scanning for 10 min were also monitored. As shown in Figure S14 in the Supporting Information, the intensity decreases in both the CLSM and TPM fluorescence images are less than 20% of its original intensity (estimated by using ImageJ), which indicate good photostability of TVFVBN-S-NH₂FA in the cellular environment.

Conclusion

In summary, we have synthesized glucopyranose functionalized star-shaped conjugated oligomers with a push-pull structure for two-photon fluorescence imaging. The precursor oligomer TVFVBN-S-NH₂ has been found to self-assemble into nanoparticles with a quantum yield of 0.21 in water. These nanoparticles have a large TPA cross-section of ~1100 GM at 780 nm in aqueous solution when calculated based on a molecule. More importantly, this glycosylated material is born with a reactive amine group on each glucopyranose substituent, which allows further modification with versatile biocompatible elements or bio-recognition moieties. As a demonstration, folic acid was conjugated to TVFVBN-S-NH₂ to yield TVFVBN-S-NH₂FA, which shows similar self-assembly behaviour and optical properties as those of TVFVBN-S-NH₂. Cellular studies reveal that both nanoparticles show low cytotoxicity and TVFVBN-S-NH₂FA is more favourable to MCF-7 cells due to specific folic acid-folate receptor interactions on cell membranes. As a result, this study highlights the glycosylation strategy as an effective molecular engineering approach to develop robust materials with good water dispersibility, self-assembly ability and large TPA cross-sections for targeted cancer cell imaging.

Experimental Section

Materials and instruments: Chemicals and reagents were purchased from Sigma-Aldrich unless otherwise stated. NMR spectra were collected on a Bruker AMX 500 spectrometer with [D]chloroform as the solvent (unless otherwise stated) and tetramethylsilane as the internal standard. Elemental analyses were carried out by the Microanalysis Laboratory of the National University of Singapore. UV/Vis spectra were recorded on a Shimadzu UV-1700 spectrometer. Fluorescence measurements were

carried out on a Perkin-Elmer LS-55 instrument equipped with a xenon-lamp excitation source and a Hamamatsu (Japan) 928 photomultiplier tube (PMT), by using 90° angle detection for solution samples. Quantum yields were measured by using Rhodamine 6G in methanol as the reference.

2-*p*-Tolylbenzo[*d*]thiazole (1): A mixture of 4-methylbenzaldehyde (7 mL, 58 mmol), 2-aminothiophenol (7 mL, 65 mmol), and NMP (50 mL) was heated in an oil bath at a temperature of 110°C for 72 h, which was then poured into 1:1 ethanol/water. The precipitates were collected and recrystallized from ethanol to afford **1** as yellow needle crystals (11 g, 84%). ¹H NMR (500 MHz, CDCl₃): δ = 8.06 (d, *J* = 8 Hz, 1H), 7.99 (d, *J* = 8.5 Hz, 2H), 7.89 (d, *J* = 8 Hz, 1H), 7.49 (t, *J* = 7 Hz, 1H), 7.37 (t, *J* = 8 Hz, 1H), 7.29 (d, *J* = 8 Hz, 2H), 2.43 ppm (s, 3H); ¹³C NMR (125 MHz, CDCl₃): δ = 168.25, 154.19, 141.44, 134.98, 131.00, 129.74, 127.52, 126.26, 125.02, 123.08, 121.58, 21.54 ppm; MS (EI): *m/z*: 225.1 [*M*⁺].

2-(4-(Bromomethyl)phenyl)benzo[*d*]thiazole (2): 2-*p*-Tolylbenzo[*d*]thiazole (**1**) (1.5 g, 6.7 mmol) and NBS (1.2 g, 6.7 mmol) were mixed in CCl₄ (40 mL). The suspension was irradiated to reflux under a 120 W lamp for 1 h. Completion of reaction was confirmed by TLC. After cooling down to room temperature, the succinimide salt was filtered off and solvent was removed under reduced pressure. The residue was dissolved in dichloromethane and washed with water three times. The organic layer was dried with MgSO₄ and solvent was subsequently removed under reduced pressure. The crude product was recrystallized from ethanol to yield **2** as white crystals (1.4 g, 64%). ¹H NMR (500 MHz, CDCl₃): δ = 8.09–8.06 (m, 3H), 7.90 (d, *J* = 8 Hz, 1H), 7.51–7.48 (m, 3H), 7.40 (t, *J* = 8 Hz, 1H), 4.53 ppm (s, 2H); ¹³C NMR (125 MHz, CDCl₃): δ = 167.13, 154.16, 140.58, 135.13, 133.66, 129.68, 126.43, 125.37, 123.37, 121.65, 32.55 ppm; MS (EI): *m/z*: 303.0 [*M*⁺], 305.0 [*M*⁺], 224.1 [*M*⁺–Br].

Diethyl (4-(benzo[*d*]thiazol-2-yl)phenyl)methylphosphonate (3): 2-(4-(Bromomethyl)phenyl)benzo[*d*]thiazole (**2**) (1.2 g, 4 mmol) and triethylphosphite (1.0 g, 6 mmol) were mixed and heated at 180°C for 3 h under an argon atmosphere. After cooling down to 50°C, excess of triethylphosphite was distilled off under vacuum. The crude yellow solid product was dissolved in diethyl ether and precipitated in hexane to afford **3** as white needle crystals (1.2 g, 84%). ¹H NMR (500 MHz, CDCl₃): δ = 8.11–8.07 (m, 3H), 7.93 (d, *J* = 8 Hz, 1H), 7.51 (t, *J* = 7.5 Hz, 1H), 7.47–7.45 (m, 2H), 7.42 ppm (t, *J* = 7 Hz, 1H); ¹³C NMR (125 MHz, CDCl₃): δ = 167.68, 154.16, 135.09, 135.05, 135.02, 132.37, 132.34, 130.46, 130.41, 127.72, 127.69, 126.33, 125.19, 123.21, 121.60, 62.30, 62.25, 34.47, 33.38, 16.41, 16.36 ppm; MS (EI): *m/z*: 361.1 [*M*⁺], 224.0 [*M*⁺–C₄H₁₀O₃P].

Tris(4-formylphenyl)amine (4): Phosphorus oxychloride (9.5 mL, 101.9 mmol) was added dropwise to dry DMF (7.3 mL, 94.3 mmol) at 0°C under an argon atmosphere. The mixture was stirred at 0°C for 1 h and additionally stirred at room temperature for 1 h. After the addition of triphenylamine (5.0 g, 20.4 mmol) in chloroform (5 mL), the mixture was stirred at 100°C overnight. After cooling, the solution was poured into ice water (400 mL) and the resulting mixture was neutralized to pH 7 with 5% NaOH aqueous solution. After extraction with dichloromethane, the organic layer was washed with brine and water three times. The organic layer was dried with MgSO₄ and solvent was removed under reduced pressure. The residue was filtered through a short column with hexane/dichloromethane (1:2, v/v) to produce yellowish solids. After drying, the solid was added into an ice-cooled mixture of phosphorus oxychloride (9.5 mL, 101.9 mmol) and dry DMF (7.3 mL, 94.3 mmol) under an argon atmosphere. The resulting mixture was heated at 100°C overnight. After cooling, the solution was poured into ice water (400 mL) and the resulting mixture was neutralized to pH 7 with 5% NaOH aqueous solution, which was then extracted with dichloromethane. The organic layer was washed with brine and water and then dried over MgSO₄. After the solvent was removed under reduced pressure, the residue was columned by using hexane/dichloromethane (1:4, v/v) to yield **4** as yellow crystals (2.7 g, 40%). ¹H NMR (500 MHz, CDCl₃): δ = 9.96 (s, 3H), 7.85 (d, *J* = 8.5 Hz, 6H), 7.27 ppm (d, *J* = 7 Hz, 6H); ¹³C NMR (125 MHz, CDCl₃): δ = 190.51, 151.21, 132.59, 131.52, 124.55 ppm; MS (EI): *m/z*: 329.0 [*M*⁺].

Tris(4-hydroxyphenyl)amine (5): Tris(4-formylphenyl)amine (**4**) (1.0 g, 3.0 mmol) and NaBH₄ (1.6 g, 42.6 mmol) were suspended into methanol (50 mL), which was then refluxed for 5 h. After cooling down to room temperature, the reaction solution was quenched with water. The mixture was further diluted with water (200 mL) and neutralized to pH 7 by using diluted acetic acid. White solid precipitated after neutralization, which was collected via centrifugation and dried under vacuum to give **5** as a white solid (1 g, 98%). ¹H NMR (500 MHz, CDCl₃): δ = 7.25 (d, *J* = 8.5 Hz, 6H), 7.06 (d, *J* = 8.5 Hz, 6H), 4.65 ppm (s, 6H); ¹³C NMR (125 MHz, CDCl₃): δ = 147.27, 135.31, 128.30, 124.17, 65.08 ppm; MS (EI): *m/z*: 335.2 [*M*⁺].

Tris(4-bromomethylphenyl)amine (6): HBr gas was bubbled into a suspension of tri(4-hydroxyphenyl)amine **5** (500 mg, 1.5 mmol) in CHCl₃ (200 mL) for 20 min. The resulting solution was allowed to stir at room temperature for 2 days in a sealed round-bottomed flask. Nitrogen gas was then bubbled into the solution to remove excess of HBr gas. The resulting solution was washed with saturated NaHCO₃ (150 mL) and then washed with brine before drying with MgSO₄. Solvent removal under reduced pressure gave **6** as a white solid (708 mg, 90%). ¹H NMR (500 MHz, CDCl₃): δ = 7.27 (d, *J* = 8.5 Hz, 6H), 7.03 (d, *J* = 8 Hz, 6H), 4.49 ppm (s, 6H); MS (EI): *m/z*: 524.9 [*M*⁺], 444.0 [*M*⁺ - Br].

Tris(4-diethylphosphonatemethylphenyl)amine (7): Tri(4-bromomethylphenyl)amine (**6**) (500 mg, 0.95 mmol) and triethylphosphite (712 mg, 4.3 mmol) were mixed under an argon atmosphere. The resulting mixture was heated at 120 °C overnight. After cooling down to 50 °C, the excess of triethylphosphite was removed by using vacuum distillation. The residue was dissolved in diethyl ether and poured into hexane (30 mL) to give **7** as a colourless oil (500 mg, 76%). ¹H NMR (500 MHz, CDCl₃): δ = 7.16–7.14 (m, 6H), 6.97 (d, *J* = 8.5 Hz, 6H), 4.04 (quintet, 12H), 3.09 (d, *J* = 21.5 Hz, 6H), 1.25 ppm (t, *J* = 7.5 Hz, 18H); ¹³C NMR (125 MHz, CDCl₃): δ = 146.45, 146.43, 130.66, 130.60, 125.78, 125.70, 124.08, 124.06, 62.13, 62.08, 33.64, 32.54, 16.36, 16.32 ppm; MS (EI) *m/z*: 695.4 [*M*⁺].

9,9-Bis(6-bromohexyl)-9H-fluorene-2,7-dicarbaldehyde (8): 2,7-Dibromo-9,9-di(6-bromohexyl)fluorene (3.9 g, 6.0 mmol) in freshly distilled THF (60 mL) was cooled to -78 °C with a dry ice/acetone bath under an argon atmosphere. At -78 °C, *n*BuLi in hexane (9 mL, 12.4 mmol) was added dropwise into the solution, which was stirred for 30 min. Anhydrous DMF (1.2 mL, 15 mmol) was subsequently added and the solution was stirred for another 2 h at -78 °C before being kept at room temperature overnight. The resulting mixture was quenched with water and the solvent was removed by evaporation. After extraction with dichloromethane, the organic phase was separated and dried over MgSO₄. After solvent removal under reduced pressure, the residue was purified with silica gel column by using hexane/dichloromethane (3:2, v/v) to afford **8** as a colourless oil (1.3 g, 39%), which solidified after standing in a fridge overnight. ¹H NMR (500 MHz, CDCl₃): δ = 10.07 (s, 2H), 7.92–7.88 (m, 6H), 3.20 (t, *J* = 7 Hz, 4H), 2.07–2.04 (m, 4H), 1.69–1.56 (m, 4H), 1.11–1.02 (m, 8H), 0.88–0.53 ppm (m, 4H); ¹³C NMR (125 MHz, CDCl₃): δ = 191.93, 152.51, 145.56, 136.58, 130.37, 123.33, 121.43, 55.45, 39.83, 33.69, 32.52, 28.87, 27.70, 23.59 ppm; MS (EI) *m/z*: 548.2 [*M*⁺].

7-((E)-2-[4-(Benzo[d]thiazol-2-yl)phenyl]vinyl)-9,9-bis(6-bromohexyl)-9H-fluorene-2-carbaldehyde (9): Diethyl [4-(benzo[d]thiazol-2-yl)phenyl]methylphosphonate (**3**) (200 mg, 0.55 mmol) and 9,9-bis(6-bromohexyl)-9H-fluorene-2,7-dicarbaldehyde (**8**) (274 mg, 0.50 mmol) were dissolved in freshly distilled THF (10 mL) under an argon atmosphere. The solution was cooled to -10 °C and a suspension of potassium *tert*-butoxide (140 mg, 1.24 mmol) in dry THF (5 mL) was added dropwise. The reaction was kept at -10 °C for 4 h and then quenched with water. The solvent of the mixture was removed by evaporation. After extraction with dichloromethane, the organic layer was washed with brine and water, dried with MgSO₄, and the solvent was removed under reduced pressure. The residue was columned with dichloromethane/hexane (1:1, v/v) to give **9** as a yellow solid (132 mg, 35%). ¹H NMR (500 MHz, CDCl₃): δ = 10.07 (s, 1H), 8.13–8.08 (m, 3H), 7.92 (d, *J* = 8 Hz, 1H), 7.88–7.83 (m, 3H), 7.78 (d, *J* = 7.5 Hz, 1H), 7.69 (d, *J* = 8.5 Hz, 2H), 7.60 (d, *J* = 8 Hz, 1H), 7.54–7.49 (m, 2H), 7.40 (t, *J* = 8 Hz, 1H), 7.34 (d, *J* = 16.5 Hz, 1H), 7.26 (d, *J* = 16.5 Hz, 1H), 3.27 (t, *J* = 7 Hz, 4H), 2.08–2.06 (m, 4H), 2.05–1.68 (m, 4H), 1.63–1.08 (m, 8H), 0.65–0.59 ppm (m, 4H); ¹³C NMR

(125 MHz, CDCl₃): δ = 192.19, 167.64, 154.21, 152.48, 151.47, 147.09, 139.91, 139.69, 137.80, 135.43, 135.03, 132.79, 130.87, 130.49, 128.23, 128.00, 127.10, 126.42, 126.31, 125.25, 123.20, 122.84, 121.64, 121.42, 121.08, 120.14, 55.19, 40.14, 33.82, 32.58, 28.99, 27.76, 23.57 ppm; MS (EI): *m/z*: 755.3 [*M*⁺].

***N*-Tris[4,4',4''-((E)-2-((E)-2-[4-(benzo[d]thiazol-2-yl)phenyl]vinyl)-9,9-bis(6-bromohexyl)-9H-fluorene-2-carbaldehyde (9) (100 mg, 0.13 mmol) and tris(4-diethylphosphonatemethylphenyl)amine **7** (26 mg, 0.037 mmol) was mixed in dry THF (10 mL) under an argon atmosphere, and then the solution was cooled down to 0 °C. A suspension of potassium *tert*-butoxide (19 mg, 0.17 mmol) in dry THF (5 mL) was added dropwise into the solution. The reaction was kept at 0 °C for 6 h before it was quenched with water. The solvent was removed under reduced pressure and dichloromethane was used for extraction. The organic layer was washed with brine and water and then dried with MgSO₄. After solvent removal, the residue was columned by using dichloromethane/hexane (1:1, v/v) to give TVFVBN as a yellow solid (60 mg, 65%). ¹H NMR (500 MHz, CDCl₃): δ = 8.12–8.07 (m, 9H), 7.91 (d, *J* = 8.5 Hz, 3H), 7.69–7.67 (m, 12H), 7.56–7.47 (m, 21H), 7.40 (t, *J* = 6 Hz, 3H), 7.33 (d, *J* = 15.5 Hz, 3H), 7.24–7.17 (m, 15H), 3.28 (t, *J* = 7.5 Hz, 12H), 2.07–2.04 (m, 12H), 1.69–1.64 (m, 12H), 1.24–1.13 (m, 24H), 0.88–0.86 ppm (m, 12H); ¹³C NMR (125 MHz, CDCl₃): δ = 167.71, 154.28, 151.32, 151.28, 141.21, 140.34, 140.25, 138.92, 136.85, 135.96, 135.06, 132.52, 130.98, 129.06, 127.98, 127.05, 126.97, 126.39, 126.16, 125.71, 125.19, 124.35, 123.19, 121.64, 120.93, 120.60, 120.18, 120.10, 114.11, 54.96, 40.38, 34.02, 32.65, 29.09, 27.77, 23.59 ppm; MS (MALDI-TOF): *m/z*: calcd for C₁₄₄H₁₃₈Br₆N₃S₃ [*M*⁺]: 2500.5; found: 2500.5.**

***N*-Tris[4,4',4''-((E)-2-((E)-2-[4-(benzo[d]thiazol-2-yl)phenyl]vinyl)-9,9-bis(6-2-acetamido-2-deoxy-1-thio-β-D-glucopyranose 3,4,6-triacetate-hexyl)-9H-fluorene-7-yl)vinyl]phenyl]phenylamine (TVFVBN-S-NHAc):** *N*-Tris[4,4',4''-((E)-2-((E)-2-[4-(benzo[d]thiazol-2-yl)phenyl]vinyl)-9,9-bis(6-bromohexyl)-9H-fluorene-7-yl)vinyl]phenyl]phenylamine (TVFVBN) (30 mg, 0.012 mmol), 2-acetamido-2-deoxy-1-thio-β-D-glucopyranose 3,4,6-triacetate (52 mg, 0.14 mmol) and K₂CO₃ (200 mg, 1.4 mmol) were mixed in THF (5 mL). The mixture was stirred at room temperature for 3 days. The solvent was removed and the residue was dissolved with dichloromethane. After washing with brine and water and drying with MgSO₄, the solvent was removed under reduced pressure. Gradient column chromatography firstly by using ethyl acetate to remove an excess of 2-acetamido-2-deoxy-1-thio-β-D-glucopyranose 3,4,6-triacetate, then ethyl acetate/methanol (10:1, v/v) to give TVFVBN-S-NHAc as a yellow solid after precipitation from methanol (40 mg, 80%). ¹H NMR (500 MHz, CDCl₃): δ = 8.11 (d, *J* = 8 Hz, 2H), 8.08 (d, *J* = 8.5 Hz, 1H), 7.91 (d, *J* = 8 Hz, 1H), 7.69 (m, 4H), 7.56–7.46 (m, 7H), 7.40–7.36 (m, 2H), 7.25–7.17 (m, 5H), 5.57–5.51 (m, 2H), 5.14–5.01 (m, 4H), 4.47–4.43 (m, 2H), 4.18–3.99 (m, 6H), 3.58–3.54 (m, 2H), 2.58–2.52 (m, 4H), 2.00–1.98 (m, 22H), 1.87 (m, 6H), 1.43–1.40 (m, 4H), 1.17–1.11 (m, 8H), 0.69–0.66 ppm (m, 4H); ¹³C NMR (125 MHz, CDCl₃): δ = 171.04, 170.63, 170.01, 169.29, 167.69, 154.16, 151.42, 140.24, 134.99, 128.00, 127.01, 126.42, 125.22, 123.14, 121.63, 120.93, 84.41, 75.80, 73.87, 68.49, 62.31, 54.97, 53.27, 40.47, 33.39, 29.80, 29.37, 29.28, 28.38, 28.27, 23.46, 23.20, 20.69, 20.62 ppm; MS (MALDI-TOF): *m/z*: calcd for C₂₂₈H₂₅₈N₁₀O₄₈S₉: 4193.56 [*M*⁺]; found: 4193.34.

***N*-Tris[4,4',4''-((E)-2-((E)-2-[4-(benzo[d]thiazol-2-yl)phenyl]vinyl)-9,9-bis(6-2-amido-2-deoxy-1-thio-β-D-glucopyranose-hexyl)-9H-fluorene-7-yl)vinyl]phenyl]phenylamine (TVFVBN-S-NH₂):** *N*-Tris[4,4',4''-((E)-2-((E)-2-[4-(benzo[d]thiazol-2-yl)phenyl]vinyl)-9,9-bis(6-2-acetamido-2-deoxy-1-thio-β-D-glucopyranose 3,4,6-triacetate-hexyl)-9H-fluorene-7-yl)vinyl]phenyl]phenylamine (TVFVBN-S-NHAc) (20 mg, 0.0047 mmol) and hydrazine monohydrate (1 mL) were heated at 120 °C in a sealed tube for 2 days. After cooling down to room temperature, the reaction mixture was purified by dialysis against Mill-Q water by using a 3.5 kDa molecular weight cut-off dialysis membrane for 3 days. It was then lyophilized to give TVFVBN-S-NH₂ as a yellow solid (14 mg, 94%). ¹H NMR (500 MHz, DMSO): δ = 8.10 (d, *J* = 7.5 Hz, 1H), 8.01 (d, *J* = 7.5 Hz, 1H), 7.49 (d, *J* = 7 Hz, 2H), 7.65–7.60 (m, 4H), 7.52 (t, *J* = 7.5 Hz,

1H), 7.45 (t, $J=8$ Hz, 1H), 7.35 (d, $J=6.5$ Hz, 2H), 7.15 (m, 8H), 6.81 (m, 2H), 4.98–4.94 (m, 2H), 4.45–4.10 (m, 4H), 3.62–3.60 (m, 2H), 3.06–2.83 (m, 14H), 2.41–2.40 (m, 4H), 1.82–1.80 (m, 4H), 1.23 (m, 4H), 0.99–0.91 (m, 8H), 0.40 ppm (m, 4H).

Synthesis of TVFVBN-S-NH₂FA: The conjugation of TVFVBN-S-NH₂ with folic acid was carried out through a DCC/NHS coupling reaction. In brief, folic acid (1 mmol) in DMSO (20 mL) was activated by using DCC (1.2 mmol) and NHS (2 mmol) at 50 °C for 6 h. After the reaction, the insoluble salt was filtered off. The resulting folate-NHS solution (2 μ L, containing 1×10^{-4} mmol of folate-NHS) was added into TVFVBN-S-NH₂ (3 mg, 1×10^{-3} mmol) in DMSO (1 mL), together with a catalytic amount of pyridine. The reaction mixture was stirred overnight at room temperature. The resulting solution was dialyzed by using a 3.5 kDa molecular weight cut-off dialysis membrane for 2 days to eliminate the unreacted folate-NHS. TVFVBN-S-NH₂FA was finally collected after lyophilisation in a quantitative yield.

Cell culture and incubation: MCF-7 breast cancer cells were cultured in Dulbecco's Modified Eagle Medium (DMEM) medium containing 10% fetal bovine serum and 1% penicillin-streptomycin at 37 °C in a humidified environment containing 5% CO₂. Before experiments, the cells were precultured until confluence was reached.

Cell viability: MTT assays were performed to assess the metabolic activity of MCF-7 breast cancer cells. MCF-7 cells were seeded in 96-well plates (Costar, IL, USA) at an intensity of 2×10^4 cells mL⁻¹. After 48 h incubation, the medium was replaced by TVFNBN-S-NH₂ and TVFNBN-S-NH₂FA solutions at concentrations of 1 and 3 μ M, and the cells were then incubated for 24, 48 and 72 h, respectively. After the designated time intervals, the wells were washed twice with $1 \times$ PBS buffer and freshly prepared MTT (100 μ L, 0.5 mg mL⁻¹) solution in culture medium was added into each well. The MTT medium solution was carefully removed after 3 h incubation in the incubator.

Isopropanol (100 μ L) was then added into each well and the plate was gently shaken for 10 min at room temperature to dissolve all the precipitate formed. The absorbance of MTT at 570 nm was monitored by the microplate reader (Genios Tecan). Cell viability was expressed by the ratio of the absorbance of the cells incubated with TVFNBN-S-NH₂ and TVFNBN-S-NH₂FA solutions to that of the cells incubated with culture medium only.

One- and two-photon fluorescence imaging: MCF-7 cells and NIH/3T3 cells were cultured in a chamber (LAB-TEK, Chambered Coverglass System) at 37 °C for qualitative study. After 80% confluence, the medium was removed and the adherent cells were washed twice with $1 \times$ PBS buffer. TVFNBN-S-NH₂ and TVFNBN-S-NH₂FA solutions (0.8 mL, 1 μ M) were then added to the chambers. After incubation for 2 h, cells were washed three times with $1 \times$ PBS buffer and then fixed by 75% ethanol for 20 min, which was further washed with $1 \times$ PBS buffer twice. The nuclei were stained with propidium iodide (PI) for 40 min. The cells were then imaged by CLSM (Zeiss LSM 410, Jena, Germany) with imaging software (Fluoview FV1000). TVFNBN-S-NH₂ and TVFNBN-S-NH₂FA were excited at 405 nm (3% laser power), and the fluorescence was collected from 505–560 nm. PI was excited at 543 nm and the fluorescence was collected at 575–635 nm. To study the competitive effect of free folic acid on the endocytosis of TVFVBN-S-NH₂FA, 50 μ g mL⁻¹ free folic acid in medium was first added into the chamber. After 30 min, the medium was replaced by 1 μ M TVFVBN-S-NH₂FA and incubated for 2 h before imaging.

To obtain two-photon images, the cells (without nuclei stained) were imaged with multiphoton microscopes (Leica TCS SP5 X) with a Leica HCX PL APO 63x/1.20 W CORR CS objective lens. The probes were excited with a mode-locked Ti:Sapphire laser source (Chameleon Ultra II) with 10 mW average power in the focal plane. Internal PMTs were used to collect the signals at 505–560 nm in an 8 bit unsigned 1024 \times 1024 pixels at 400 Hz scan speed.

Acknowledgements

The authors are grateful to the Singapore National Research Foundation (R279-000-323-281), the Temasek Defence Systems Institute (R279-000-305-232/422/592) and the Institute of Materials Research and Engineering (IMRE/11-1C0213) for financial support.

- [1] a) C. Xu, W. Zipfel, J. B. Shear, R. M. Williams, W. W. Webb, *Proc. Nat. Acad. Sci. USA* **1996**, *93*, 10763–10768; b) E. Gratton, *Science* **2011**, *331*, 1016–1017; c) M. Rubart, *Circ. Res.* **2004**, *95*, 1154–1166; d) F. Helmchen, W. Denk, *Nat. Methods* **2005**, *2*, 932–940; e) W. Zipfel, R. M. Williams, W. W. Webb, *Nat. Biotechnol.* **2003**, *21*, 1369–1377; f) A. Diaspro, C. J. R. Sheppard in *Two-Photon Microscopy: Basic Principles and Architectures*, Wiley, New York, **2002**.
- [2] a) B. Dubertret, P. Skourides, D. J. Norris, V. Noireaux, A. H. Brivanlou, A. Alibchaber, *Science* **2002**, *298*, 1759–1762; b) A. M. Derfus, W. C. W. Chan, S. N. Bhatia, *Nano Lett.* **2004**, *4*, 11–18; c) A. M. Smith, H. Duan, A. M. Mohs, S. Nie, *Adv. Drug Delivery Rev.* **2008**, *60*, 1226–1240.
- [3] M. Drobizhev, N. S. Makarov, S. E. Tillo, T. E. Hughes, A. Rebane, *Nat. Methods* **2011**, *8*, 393–399.
- [4] A. Müller-Taubenberger, K. I. Anderson, *Appl. Microbiol. Biotechnol.* **2007**, *77*, 1–12.
- [5] a) M. Pawlicki, H. A. Collins, R. G. Denning, H. L. Anderson, *Angew. Chem.* **2009**, *121*, 3292–3316; *Angew. Chem. Int. Ed.* **2009**, *48*, 3244–3266; b) G. S. He, L.-S. Tan, Q. Zheng, P. N. Prasad, *Chem. Rev.* **2008**, *108*, 1245–1330.
- [6] a) C. Le Droumaguet, O. Mongin, M. H. V. Werts, M. Blanchard-Desce, *Chem. Commun.* **2005**, 2802–2804; b) S.-J. Chung, K.-S. Kim, T.-C. Lin, G. S. He, J. Swiatkiewicz, P. N. Prasad, *J. Phys. Chem. B* **1999**, *103*, 10741–10745.
- [7] a) H. Y. Woo, D. Korystov, A. Mikhailovsky, T.-O. Nguyen, G. C. Bazan, *J. Am. Chem. Soc.* **2005**, *127*, 13794–13795; b) H. Y. Woo, B. Liu, B. Kohler, D. Korystov, A. Mikhailovsky, G. C. Bazan, *J. Am. Chem. Soc.* **2005**, *127*, 14721–14729; c) W. F. Jager, A. A. Volkens, D. C. Neckers, *Macromolecules* **1995**, *28*, 8153–8158.
- [8] G. Wang, K.-Y. Pu, X. Zhang, K. Li, L. Wang, L. Cai, D. Ding, Y.-H. Lai, B. Liu, *Chem. Mater.* **2011**, *23*, 4428–4434.
- [9] a) R. Weissleder, V. Ntziachristos, *Nat. Med.* **2003**, *9*, 123–128; b) M. Ferrari, *Nat. Rev. Cancer* **2005**, *5*, 161–171; c) N. S. White, R. J. Errington, *Adv. Drug Delivery Rev.* **2005**, *57*, 17–42.
- [10] a) K. Li, J. Pan, S.-S. Feng, A. W. Wu, K.-Y. Pu, Y. Liu, B. Liu, *Adv. Funct. Mater.* **2009**, *19*, 3535–3542; b) T. Lu, J. Sun, X. Chen, P. Zhang, X. Jing, *Macromol. Biosci.* **2009**, *9*, 1059–1068.
- [11] K. Li, Y. Liu, K.-Y. Pu, S.-S. Feng, R. Zhan, B. Liu, *Adv. Funct. Mater.* **2011**, *21*, 287–294.
- [12] K.-T. Yong, J. Qian, I. Roy, H. H. Lee, E. J. Bergey, K. M. Trampusch, S. He, M. T. Swihart, A. Maitra, P. N. Prasad, *Nano Lett.* **2007**, *7*, 761–765.
- [13] V. A. Khanadeev, B. N. Khlebtsov, S. A. Staroverov, I. V. Vidyasheva, A. A. Skaptsov, E. S. Ileneva, V. A. Bogatyrev, L. A. Dykman, N. G. Khlebtsov, *J. Biophotonics* **2011**, *4*, 74–83.
- [14] a) A. R. Morales, K. J. Schafer-Hales, A. I. Marcus, K. D. Belfield, *Bioconjugate Chem.* **2008**, *19*, 2559–2567; b) A. R. Morales, C. O. Yanez, K. J. Schafer-Hales, A. I. Marcus, K. D. Belfield, *Bioconjugate Chem.* **2009**, *20*, 1992–2000; c) A. R. Morales, G. Luchita, C. O. Yanez, M. V. Bondar, O. V. Przhonskab, K. D. Belfield, *Org. Biomol. Chem.* **2010**, *8*, 2600–2608.
- [15] J.-H. Kim, Y.-S. Kim, K. Park, E. Kang, S. Lee, H. Y. Nam, K. Kim, J. H. Park, D. Y. Chi, R.-W. Park, I.-S. Kim, K. Choi, I. C. Kwon, *Biomaterials* **2008**, *29*, 1920–1930.
- [16] M. Huang, Z. Ma, E. Khor, L.-Y. Lim, *Pharm. Res.* **2002**, *19*, 1488–1494.
- [17] H. D. Han, L. S. Mangala, J. W. Lee, M. M. Shahzad, H. S. Kim, D. Shen, E. J. Nam, E. M. Mora, R. L. Stone, C. Lu, S. J. Lee, J. W. Roh, A. M. Nick, G. Lopez-Berestein, A. K. Sood, *Clin. Cancer Res.* **2010**, *16*, 3910–3922.

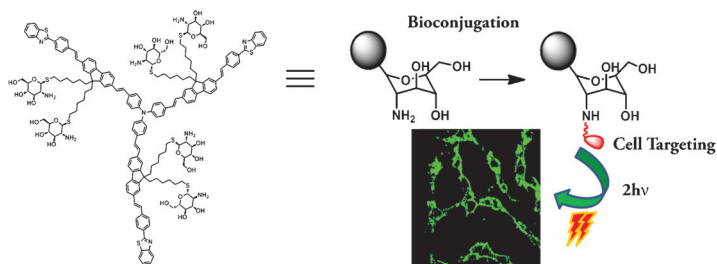
- [18] H.-Y. Wang, G. Chen, X.-P. Xu, S.-J. Ji, *Synth. Met.* **2010**, *160*, 1065–1072.
- [19] a) G. Lai, X. R. Bu, J. Santos, E. A. Mintz, *Synlett* **1997**, 1275–1276; b) T. Mallegol, S. Gmouh, M. Ait Amer Meziame, M. Blanchard-Desce, O. Mongin, *Synthesis* **2005**, 1771–1774.
- [20] a) S. Knapp, S. Gonzalez, D. S. Myers, L. L. Eckman, C. A. Bewley, *Org. Lett.* **2002**, *4*, 4337–4339; b) B. B. Metaferia, B. J. Fetterolf, S. Shazad-ul-Hussan, M. Moravec, J. A. Smith, S. Ray, M.-T. Gutierrez-Lugo, C. A. Bewley, *J. Med. Chem.* **2007**, *50*, 6326–6336; c) S. Sarkar, S. J. Sucheck, *Carbohydr. Res.* **2011**, *346*, 393–400.
- [21] a) J. Dufourcq, J. F. Faucon, G. Fourche, J. L. Dasseux, M. Le Maire, T. Gulik-Krzywicki, *Biochim Biophys Acta.* **1986**, *859*, 33–48; b) P. J. Patty, B. J. Frisken, *Biophys. J.* **2003**, *85*, 996–1004; c) P. J. Patty, B. J. Frisken, *Appl. Opt.* **2006**, *45*, 2209–2216.
- [22] a) K.-Y. Pu, K. Li, B. Liu, *Adv. Funct. Mater.* **2010**, *20*, 2770–2777; b) K.-Y. Pu, K. Li, J. Shi, B. Liu, *Chem. Mater.* **2009**, *21*, 3816–3822.
- [23] a) J. R. Lakowicz in *Principles of Fluorescence Spectroscopy*, 3rd ed., Springer Science R Business Media, LLC, New York, **2006**; b) K.-Y. Pu, B. Liu, *Adv. Funct. Mater.* **2009**, *19*, 277–284.
- [24] a) C. Xu, W. W. Webb, *J. Opt. Soc. Am. B* **1996**, *13*, 481–491; b) N. S. Makarov, M. Drobizhev, A. Rebane, *Opt. Express* **2008**, *16*, 4029–4047.
- [25] O. Mongin, L. Porrès, C. Katan, T. Pons, J. Mertz, M. Blanchard-Desce, *Tetrahedron Lett.* **2003**, *44*, 8121–8125.
- [26] E. Zojer, D. Beljonne, T. Kogej, H. Vogel, S. R. Marder, J. W. Perry, J.-L. Brédas, *J. Chem. Phys.* **2002**, *116*, 3646–3658.
- [27] a) Y. S. Tian, H. Y. Lee, C. S. Lim, J. Park, H. M. Kim, Y. N. Shin, E. S. Kim, H. J. Jeon, S. B. Park, B. R. Cho, *Angew. Chem.* **2009**, *121*, 8171–8175; *Angew. Chem. Int. Ed.* **2009**, *48*, 8027–8031; b) T. Y. Ohulchansky, H. E. Pudavari, S. M. Yarmoluk, V. M. Yashchuk, E. J. Bergey, P. N. Prasad, *Photochem. Photobiol.* **2003**, *77*, 138–145; c) C. Dyrager, A. Friberg, K. Dahlén, M. Fridén-Saxin, K. Börjesson, L. M. Wilhelmsson, M. Smedh, M. Grøtli, K. Luthman, *Chem. Eur. J.* **2009**, *15*, 9417–9423; d) R. L. McRae, R. L. Phillips, I.-B. Kim, U. H. F. Bunz, C. J. Fahrni, *J. Am. Chem. Soc.* **2008**, *130*, 7851–7853; e) D. Warther, F. Bolze, J. Léonard, S. Gug, A. Specht, D. Puliti, X.-H. Sun, P. Kessler, Y. Lutz, J.-L. Vonesch, B. Winsor, J.-F. Nicoud, M. Goeldner, *J. Am. Chem. Soc.* **2010**, *132*, 2585–2590.

Received: March 13, 2012
Published online: ■■■■, 0000

Self-Assembly

G. Wang, X. Zhang, J. Geng, K. Li,
D. Ding, K.-Y. Pu, L. Cai, Y.-H. Lai,*
B. Liu* ■■■■-■■■■

 **Glycosylated Star-Shaped Conjugated Oligomers for Targeted Two-Photon Fluorescence Imaging**



Biological imaging: A star-shaped two-photon absorbing material (see scheme) with folic acid functionaliza-

tion has been synthesized for targeted two-photon fluorescence imaging of MCF-7 cancer cells.